Uncertainty in wave propagation and imaging in random media

Josselin Garnier (Ecole Polytechnique)
http://www.josselin-garnier.org/

Sensor array imaging and (some of) its main limitations

• Sensor array imaging (echography in medical imaging, sonar, non-destructive testing, seismic exploration, etc) has two steps:
- data acquisition: an unknown medium is probed with waves; waves are emitted by a source (or a source array) and recorded by a receiver array.
- data processing: the recorded signals are processed to identify the quantities of interest (source locations, reflector locations, etc).

• Example:

Ultrasound echography

$\longrightarrow$

• Standard imaging techniques require:
- controlled and known sources,
- suitable conditions for wave propagation (ideally, homogeneous medium).

Ultrasound echography in concrete

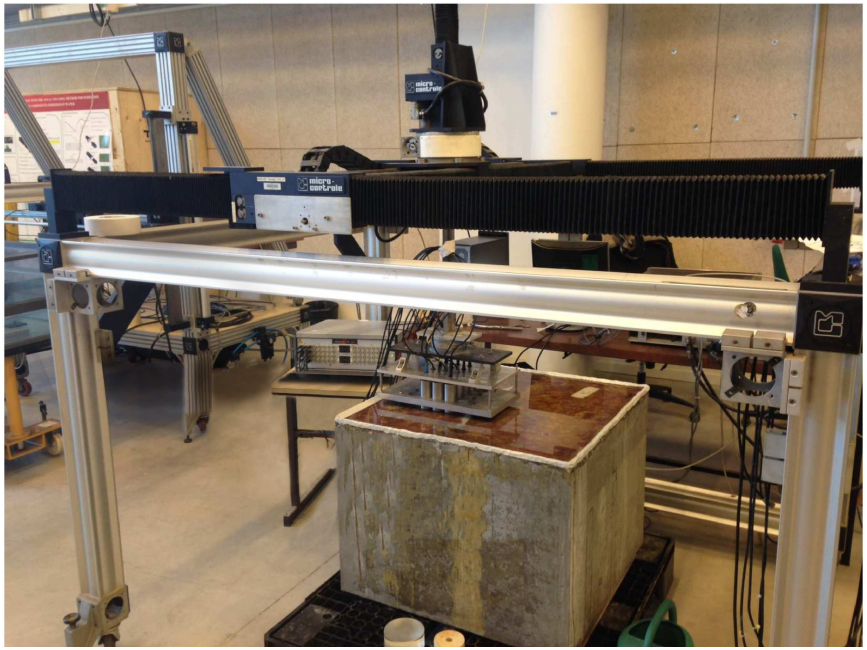

Experimental set-up

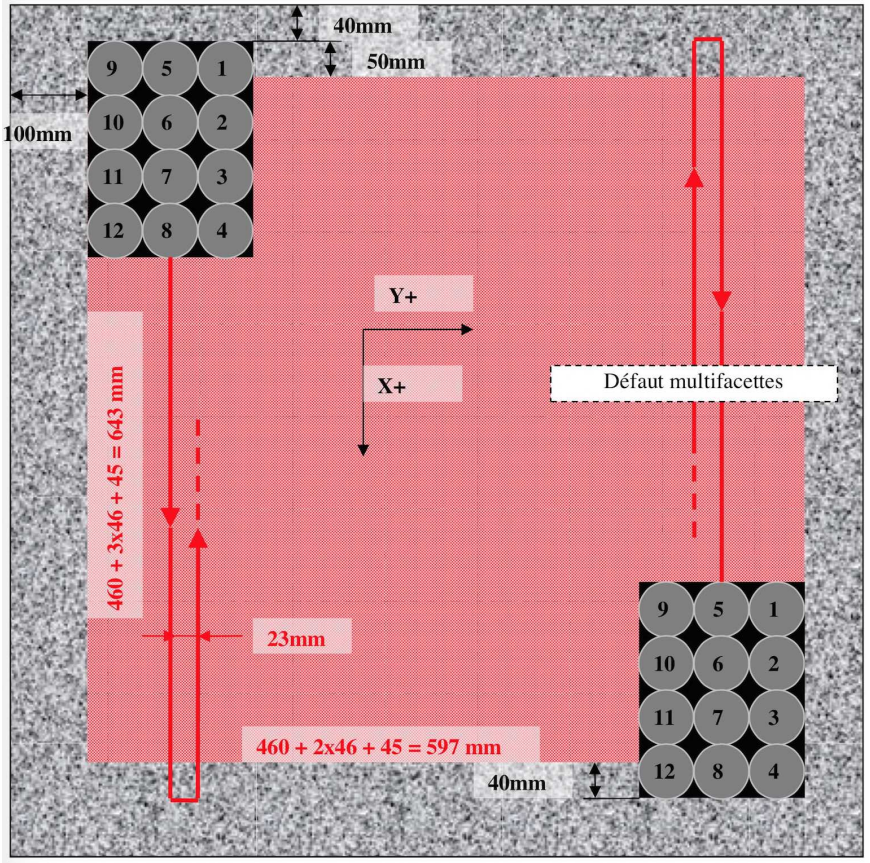

Acquisition geometry (top view)

Concrete: highly scattering medium for ultrasonic waves.

Ultrasound echography in concrete

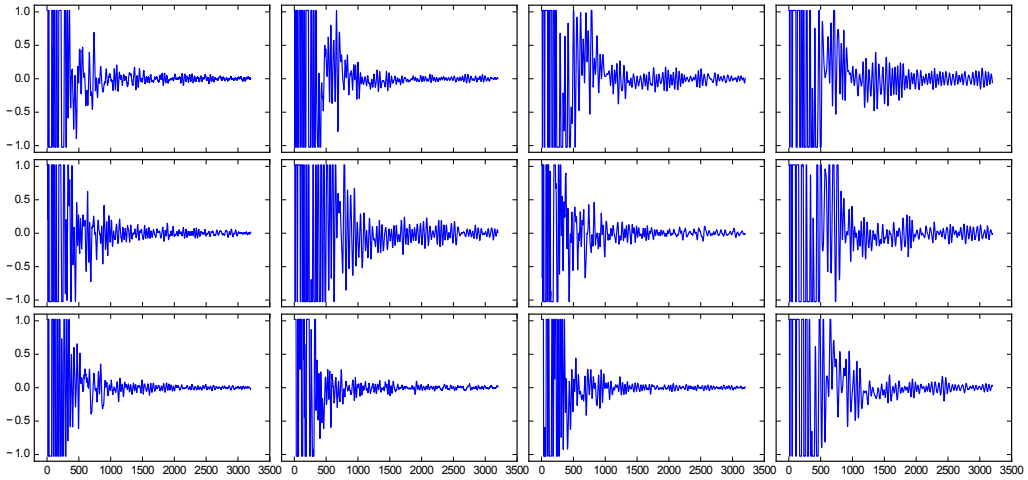

$\xrightarrow{?}$

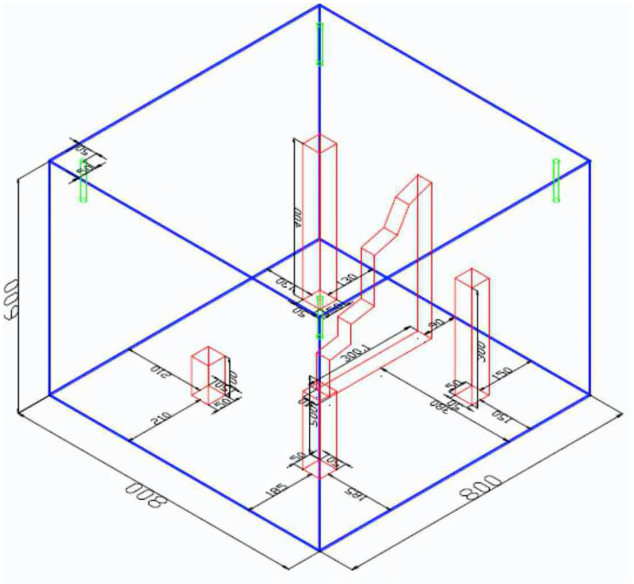

Data

Real configuration

The recorded signals are very “noisy” due to scattering.

$\hookrightarrow$ Standard imaging techniques fail.

Wave propagation in random media

- Wave equation:

$$\frac{1}{c^2(\vec{\boldsymbol{x}})}\frac{\partial^2 u}{\partial t^2}(t,\vec{\boldsymbol{x}}) - \Delta_{\vec{\boldsymbol{x}}} u(t,\vec{\boldsymbol{x}}) = F(t,\vec{\boldsymbol{x}})$$

- Time-harmonic source in the plane $z = 0$: $F(t,\vec{\boldsymbol{x}}) = \delta(z) f(\boldsymbol{x}) e^{-i\omega t}$ (with $\vec{\boldsymbol{x}} = (\boldsymbol{x}, z)$).

- Random medium model:

$$\frac{1}{c^2(\vec{\boldsymbol{x}})} = \frac{1}{c_o^2}\big(1 + \mu(\vec{\boldsymbol{x}})\big)$$

c_o is a reference speed,

$\mu(\vec{\boldsymbol{x}})$ is a zero-mean random process.

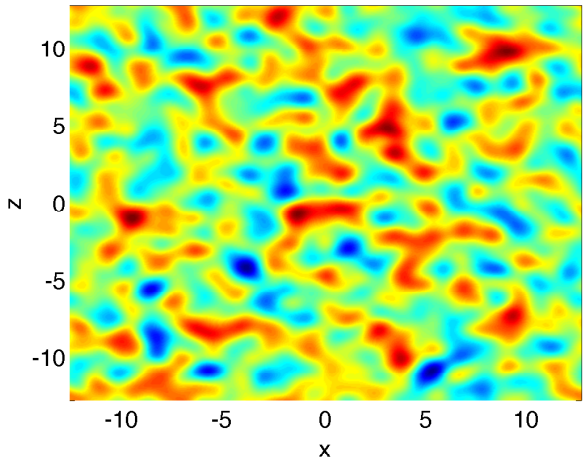

Wave propagation in the random paraxial regime

- Consider the time-harmonic wave equation (with $\vec{\boldsymbol{x}} = (\boldsymbol{x}, z)$ and $\Delta = \Delta_\perp + \partial_z^2$)

$$(\Delta_\perp + \partial_z^2)\hat{u} + \frac{\omega^2}{c_o^2}\big(1 + \mu(\boldsymbol{x}, z)\big)\hat{u} = -\delta(z) f(\boldsymbol{x}).$$

Consider the paraxial regime "$\lambda \ll l_c, r_o \ll L$":

$$\omega \to \frac{\omega}{\varepsilon^4}, \qquad \mu(\boldsymbol{x}, z) \to \varepsilon^3 \mu\big(\frac{\boldsymbol{x}}{\varepsilon^2}, \frac{z}{\varepsilon^2}\big), \qquad f(\boldsymbol{x}) \to f\big(\frac{\boldsymbol{x}}{\varepsilon^2}\big).$$

The function $\hat{\phi}^\varepsilon$ (slowly-varying envelope of a plane wave) defined by

$$\hat{u}^\varepsilon(\omega, \boldsymbol{x}, z) = \frac{i\varepsilon^4 c_o}{2\omega} \exp\big(i\frac{\omega z}{\varepsilon^4 c_o}\big)\hat{\phi}^\varepsilon\big(\omega, \frac{\boldsymbol{x}}{\varepsilon^2}, z\big)$$

satisfies

$$\varepsilon^4 \partial_z^2 \hat{\phi}^\varepsilon + \left(2i\frac{\omega}{c_o}\partial_z \hat{\phi}^\varepsilon + \Delta_\perp \hat{\phi}^\varepsilon + \frac{\omega^2}{c_o^2}\frac{1}{\varepsilon}\mu\big(\boldsymbol{x}, \frac{z}{\varepsilon^2}\big)\hat{\phi}^\varepsilon\right) = 2i\frac{\omega}{c_o}\delta(z) f(\boldsymbol{x}).$$

[1] J. Garnier and K. Sølna, *Ann. Appl. Probab.* **19**, 318 (2009).

Wave propagation in the random paraxial regime

• Consider the time-harmonic wave equation (with $\vec{\boldsymbol{x}} = (\boldsymbol{x}, z)$ and $\Delta = \Delta_\perp + \partial_z^2$)

$$(\Delta_\perp + \partial_z^2)\hat{u} + \frac{\omega^2}{c_o^2}\big(1 + \mu(\boldsymbol{x}, z)\big)\hat{u} = -\delta(z) f(\boldsymbol{x}).$$

Consider the paraxial regime "$\lambda \ll l_c, r_o \ll L$":

$$\omega \to \frac{\omega}{\varepsilon^4}, \qquad \mu(\boldsymbol{x}, z) \to \varepsilon^3 \mu\big(\frac{\boldsymbol{x}}{\varepsilon^2}, \frac{z}{\varepsilon^2}\big), \qquad f(\boldsymbol{x}) \to f\big(\frac{\boldsymbol{x}}{\varepsilon^2}\big).$$

The function $\hat{\phi}^\varepsilon$ (slowly-varying envelope of a plane wave) defined by

$$\hat{u}^\varepsilon(\omega, \boldsymbol{x}, z) = \frac{i\varepsilon^4 c_o}{2\omega} \exp\big(i\frac{\omega z}{\varepsilon^4 c_o}\big)\hat{\phi}^\varepsilon\big(\omega, \frac{\boldsymbol{x}}{\varepsilon^2}, z\big)$$

satisfies

$$\varepsilon^4 \partial_z^2 \hat{\phi}^\varepsilon + \left(2i\frac{\omega}{c_o}\partial_z \hat{\phi}^\varepsilon + \Delta_\perp \hat{\phi}^\varepsilon + \frac{\omega^2}{c_o^2}\frac{1}{\varepsilon}\mu\big(\boldsymbol{x}, \frac{z}{\varepsilon^2}\big)\hat{\phi}^\varepsilon\right) = 2i\frac{\omega}{c_o}\delta(z) f(\boldsymbol{x}).$$

• $\hat{\phi}^\varepsilon$ converges in distribution in $C^0([0, L], L^2(\mathbb{R}^2))$ to $\hat{\phi}$ that is the unique solution of the Itô-Schrödinger equation [1]

$$d\hat{\phi} = \frac{ic_o}{2\omega}\Delta_\perp \hat{\phi} dz + \frac{i\omega}{2c_o}\hat{\phi} \circ dB(\boldsymbol{x}, z)$$

with $B(\boldsymbol{x}, z)$ Brownian field $\mathbb{E}[B(\boldsymbol{x}, z)B(\boldsymbol{x}', z')] = \gamma(\boldsymbol{x} - \boldsymbol{x}')\ \min(z, z')$,
$\gamma(\boldsymbol{x}) = \int_{-\infty}^{\infty} \mathbb{E}[\mu(\boldsymbol{0}, 0)\mu(\boldsymbol{x}, z)]dz$, and $\hat{\phi}(z = 0, \boldsymbol{x}) = f(\boldsymbol{x})$.

[1] J. Garnier and K. Sølna, *Ann. Appl. Probab.* **19**, 318 (2009).

Moment calculations in the random paraxial regime

Consider

$$d\hat{\phi} = \frac{ic_o}{2\omega}\Delta_\perp \hat{\phi} dz + \frac{i\omega}{2c_o}\hat{\phi} \circ dB(\boldsymbol{x}, z)$$

starting from $\hat{\phi}(\boldsymbol{x}, z = 0) = f(\boldsymbol{x})$.

- By Itô's formula,

$$\frac{d}{dz}\mathbb{E}[\hat{\phi}] = \frac{ic_o}{2\omega}\Delta_\perp \mathbb{E}[\hat{\phi}] - \frac{\omega^2 \gamma(\mathbf{0})}{8c_o^2}\mathbb{E}[\hat{\phi}]$$

and therefore

$$\mathbb{E}\big[\hat{\phi}(\boldsymbol{x}, z)\big] = \hat{\phi}_{\rm hom}(\boldsymbol{x}, z) \exp\Big(- \frac{\gamma(\mathbf{0})\omega^2 z}{8c_o^2}\Big),$$

where

$$\gamma(\boldsymbol{x}) = \int_{-\infty}^{\infty} \mathbb{E}[\mu(\mathbf{0}, 0)\mu(\boldsymbol{x}, z)]dz$$

and $\hat{\phi}_{\rm hom}$ is the solution in the homogeneous medium.

- Strong damping of the coherent wave.

$\Longrightarrow$ Identification of the *scattering mean free path* $Z_{\rm sca} = \frac{8c_o^2}{\gamma(\mathbf{0})\omega^2}$.

$\Longrightarrow$ Coherent imaging methods (such as Kirchhoff migration, Reverse-Time migration) fail.

Moment calculations in the random paraxial regime

• The mean Wigner transform defined by

$$W(\boldsymbol{r},\boldsymbol{\xi},z)=\int_{\mathbb{R}^2}\exp\big(-i\boldsymbol{\xi}\cdot\boldsymbol{q}\big)\mathbb{E}\left[\hat{\phi}\big(\boldsymbol{r}+\frac{\boldsymbol{q}}{2},z\big)\overline{\hat{\phi}}\big(\boldsymbol{r}-\frac{\boldsymbol{q}}{2},z\big)\right]d\boldsymbol{q},$$

is the angularly-resolved mean wave energy density.

By Itô's formula, it solves a *radiative transport-like equation*

$$\frac{\partial W}{\partial z}+\frac{c_o}{\omega}\boldsymbol{\xi}\cdot\nabla_{\boldsymbol{r}}W=\frac{\omega^2}{4(2\pi)^2c_o^2}\int_{\mathbb{R}^2}\hat{\gamma}(\boldsymbol{\kappa})\Big[W(\boldsymbol{\xi}-\boldsymbol{\kappa})-W(\boldsymbol{\xi})\Big]d\boldsymbol{\kappa},$$

starting from $W(\boldsymbol{r},\boldsymbol{\xi},z=0)=W_0(\boldsymbol{r},\boldsymbol{\xi})$, the Wigner transform of the initial field f.

• The fields at nearby points are correlated and their correlations contain information about the medium.

$\Longrightarrow$ One should use (migrate) cross correlations for imaging in random media.

Beyond the second-order moments

- Fourth-order moments are useful to:
- quantify the statistical stability of correlation-based imaging methods.
- implement intensity-correlation-based imaging methods when only intensities can be measured (optics).

Moment calculations in the random paraxial regime

- Consider

$$d\hat{\phi} = \frac{ic_o}{2\omega}\Delta_\perp \hat{\phi} dz + \frac{i\omega}{2c_o}\hat{\phi} \circ dB(\boldsymbol{x}, z)$$

starting from $\hat{\phi}(\boldsymbol{x}, z = 0) = f(\boldsymbol{x})$.

- Let us consider the fourth-order moment:

$$\begin{aligned} M_4(\boldsymbol{r}_1, \boldsymbol{r}_2, \boldsymbol{q}_1, \boldsymbol{q}_2, z) &= \mathbb{E}\Big[\hat{\phi}\big(\frac{\boldsymbol{r}_1 + \boldsymbol{r}_2 + \boldsymbol{q}_1 + \boldsymbol{q}_2}{2}, z\big)\hat{\phi}\big(\frac{\boldsymbol{r}_1 - \boldsymbol{r}_2 + \boldsymbol{q}_1 - \boldsymbol{q}_2}{2}, z\big) \\ &\quad \times \overline{\hat{\phi}}\big(\frac{\boldsymbol{r}_1 + \boldsymbol{r}_2 - \boldsymbol{q}_1 - \boldsymbol{q}_2}{2}, z\big)\overline{\hat{\phi}}\big(\frac{\boldsymbol{r}_1 - \boldsymbol{r}_2 - \boldsymbol{q}_1 + \boldsymbol{q}_2}{2}, z\big)\Big] \end{aligned}$$

By Itô's formula,

$$\frac{\partial M_4}{\partial z} = \frac{ic_o}{\omega}\big(\nabla_{\boldsymbol{r}_1} \cdot \nabla_{\boldsymbol{q}_1} + \nabla_{\boldsymbol{r}_2} \cdot \nabla_{\boldsymbol{q}_2}\big)M_4 + \frac{\omega^2}{4c_o^2}U_4(\boldsymbol{q}_1, \boldsymbol{q}_2, \boldsymbol{r}_1, \boldsymbol{r}_2)M_4,$$

with the generalized potential

$$\begin{aligned} U_4(\boldsymbol{q}_1, \boldsymbol{q}_2, \boldsymbol{r}_1, \boldsymbol{r}_2) &= \gamma(\boldsymbol{q}_2 + \boldsymbol{q}_1) + \gamma(\boldsymbol{q}_2 - \boldsymbol{q}_1) + \gamma(\boldsymbol{r}_2 + \boldsymbol{q}_1) + \gamma(\boldsymbol{r}_2 - \boldsymbol{q}_1) \\ &\quad -\gamma(\boldsymbol{q}_2 + \boldsymbol{r}_2) - \gamma(\boldsymbol{q}_2 - \boldsymbol{r}_2) - 2\gamma(\boldsymbol{0}). \end{aligned}$$

Moment equations have been studied by many groups, in particular to prove the Gaussian conjecture [1].

[1] A. Ishimaru, *Wave Propagation and Scattering in Random Media*, Academic Press, San Diego, 1978.

Moment calculations in the random paraxial regime

Take Fourier transform:

$$\hat{M}_4(\boldsymbol{\xi}_1,\boldsymbol{\xi}_2,\boldsymbol{\zeta}_1,\boldsymbol{\zeta}_2,z) = \iiiint M_4(\boldsymbol{q}_1,\boldsymbol{q}_2,\boldsymbol{r}_1,\boldsymbol{r}_2,z) \times \exp\big(-i\boldsymbol{q}_1\cdot\boldsymbol{\xi}_1 - i\boldsymbol{r}_1\cdot\boldsymbol{\zeta}_1 - i\boldsymbol{q}_2\cdot\boldsymbol{\xi}_2 - i\boldsymbol{r}_2\cdot\boldsymbol{\zeta}_2\big)d\boldsymbol{r}_1 d\boldsymbol{r}_2 d\boldsymbol{q}_1 d\boldsymbol{q}_2.$$

- In the regime "$\lambda \ll l_c \ll r_o \ll L$" [1]

$$\hat{M}_4(\boldsymbol{\xi}_1,\boldsymbol{\xi}_2,\boldsymbol{\zeta}_1,\boldsymbol{\zeta}_2,z) \simeq \Phi(K,A,f)(\boldsymbol{\xi}_1,\boldsymbol{\xi}_2,\boldsymbol{\zeta}_1,\boldsymbol{\zeta}_2,z)$$

in $C^0([0,L],L^1(\mathbb{R}^2\times\mathbb{R}^2\times\mathbb{R}^2\times\mathbb{R}^2))$, where

$$K(z) = (2\pi)^8 \exp\Big(-\frac{\omega^2}{2c_o^2}\gamma(\mathbf{0})z\Big),$$

$$A(\boldsymbol{\xi},\boldsymbol{\zeta},z) = \frac{1}{2(2\pi)^2}\int\Big[\exp\Big(\frac{\omega^2}{4c_o^2}\int_0^z \gamma\big(\boldsymbol{x}+\frac{c_o\boldsymbol{\zeta}}{\omega}z'\big)dz'\Big)-1\Big]\exp\big(-i\boldsymbol{\xi}\cdot\boldsymbol{x}\big)d\boldsymbol{x}.$$

[1] J. Garnier and K. Sølna, *ARMA* **220** (2016) 37.

Scintillation

Assume that $f(\boldsymbol{x}) = \exp\big(-\frac{|\boldsymbol{x}|^2}{2r_o^2}\big)$.

- The scintillation index defined as:

$$S(\boldsymbol{r},z) := \frac{\mathbb{E}\Big[\big|\hat{\phi}(\boldsymbol{r},z)\big|^4\Big] - \mathbb{E}\Big[\big|\hat{\phi}(\boldsymbol{r},z)\big|^2\Big]^2}{\mathbb{E}\Big[\big|\hat{\phi}(\boldsymbol{r},z)\big|^2\Big]^2}$$

satisfies:

$$S(\boldsymbol{r},z) = 1 - \frac{1}{\Big|\frac{1}{4\pi}\int_{\mathbb{R}^2}\exp\Big(\frac{\omega^2}{4c_o^2}\int_0^z \gamma\big(\boldsymbol{u}\frac{c_o z'}{\omega r_o}\big)dz' - \frac{|\boldsymbol{u}|^2}{4} + i\boldsymbol{u}\cdot\frac{\boldsymbol{r}}{r_o} + \frac{|\boldsymbol{r}|^2}{r_o^2}\Big)d\boldsymbol{u}\Big|^2}.$$

The physical conjecture is that $S \simeq 1$ when the propagation distance is larger than the scattering mean free path, as it should be for a (complex) Gaussian process.

Scintillation

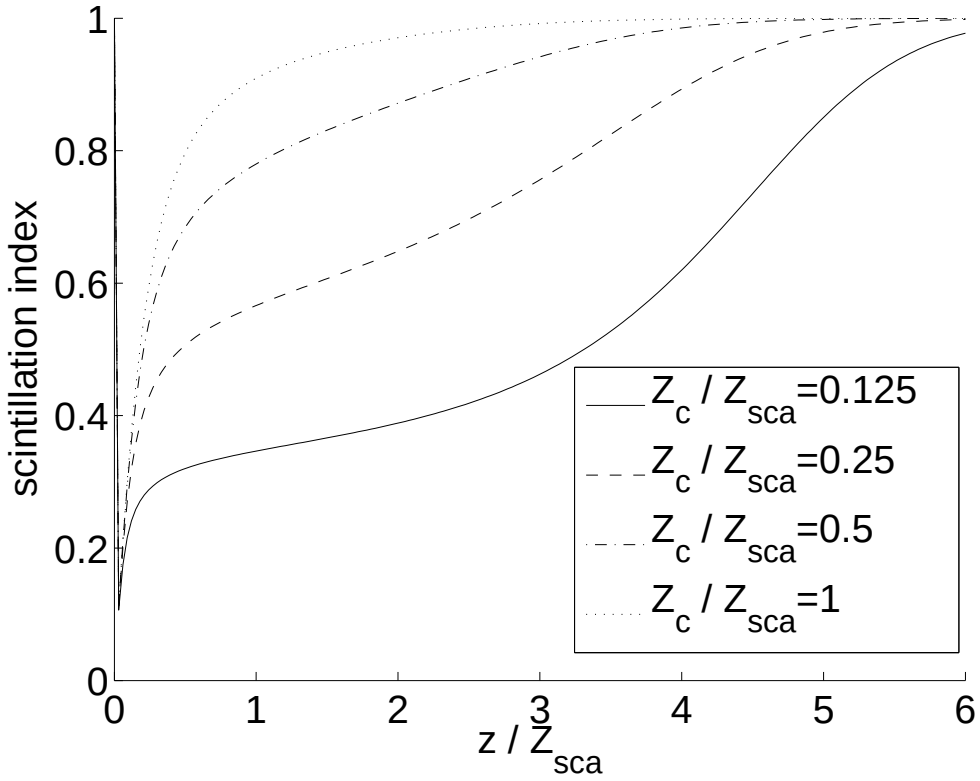

Scintillation index at the beam center $S(\mathbf{0}, z)$ as a function of the propagation distance for different values of $Z_{\rm sca} = \frac{8c_o^2}{\omega^2 \gamma(\mathbf{0})}$ and $Z_{\rm c} = \frac{\omega r_o \ell_{\rm c}}{c_o}$. Here $\gamma(\boldsymbol{x}) = \gamma(\mathbf{0}) \exp(-|\boldsymbol{x}|^2/\ell_{\rm c}^2)$.

Stability of the Wigner transform of the field

$$W(\boldsymbol{r},\boldsymbol{\xi},z) := \int_{\mathbb{R}^2} \exp\big(-i\boldsymbol{\xi}\cdot\boldsymbol{q}\big)\hat{\phi}\big(\boldsymbol{r}+\frac{\boldsymbol{q}}{2},z\big)\overline{\hat{\phi}}\big(\boldsymbol{r}-\frac{\boldsymbol{q}}{2},z\big)d\boldsymbol{q}.$$

Let us consider two positive parameters $r_{\rm s}$ and $\xi_{\rm s}$ and define the smoothed Wigner transform:

$$W_{\rm s}(\boldsymbol{r},\boldsymbol{\xi},z) = \frac{1}{(2\pi)^2 r_{\rm s}^2\xi_{\rm s}^2}\iint_{\mathbb{R}^2\times\mathbb{R}^2} W(\boldsymbol{r}-\boldsymbol{r}',\boldsymbol{\xi}-\boldsymbol{\xi}',z)\exp\Big(-\frac{|\boldsymbol{r}'|^2}{2r_{\rm s}^2}-\frac{|\boldsymbol{\xi}'|^2}{2\xi_{\rm s}^2}\Big)d\boldsymbol{r}'d\boldsymbol{\xi}'.$$

- The coefficient of variation $C_{\rm s}$ of the smoothed Wigner transform is defined by:

$$C_{\rm s}(\boldsymbol{r},\boldsymbol{\xi},z) := \frac{\sqrt{\mathbb{E}[W_{\rm s}(\boldsymbol{r},\boldsymbol{\xi},z)^2]-\mathbb{E}[W_{\rm s}(\boldsymbol{r},\boldsymbol{\xi},z)]^2}}{\mathbb{E}[W_{\rm s}(\boldsymbol{r},\boldsymbol{\xi},z)]}.$$

satisfies

$$C_{\rm s}(\boldsymbol{r},\boldsymbol{\xi},z) \simeq \left(\frac{\frac{1}{\xi_{\rm s}^2\rho_z^2}+1}{\frac{4r_{\rm s}^2}{\rho_z^2}+1}\right)^{1/2}, \qquad \rho_z^2 = \frac{\ell_{\rm c}^2}{4Z_{\rm sca}z}\frac{r_o^2+\frac{8c_o^2z^3}{3\omega^2\ell_{\rm c}^2Z_{\rm sca}}}{r_o^2+\frac{2c_o^2z^3}{3\omega^2\ell_{\rm c}^2Z_{\rm sca}}},$$

when

$$\gamma(\boldsymbol{x}) = \int_{-\infty}^{\infty}\mathbb{E}[\mu(\boldsymbol{0},0)\mu(\boldsymbol{x},z)]dz = \gamma(\boldsymbol{0})\Big[1-\frac{|\boldsymbol{x}|^2}{\ell_{\rm c}^2}+o\Big(\frac{|\boldsymbol{x}|^2}{\ell_{\rm c}^2}\Big)\Big], \qquad z\gg Z_{\rm sca}=\frac{8c_o^2}{\gamma(\boldsymbol{0})\omega^2}.$$

Stability of the Wigner transform of the field

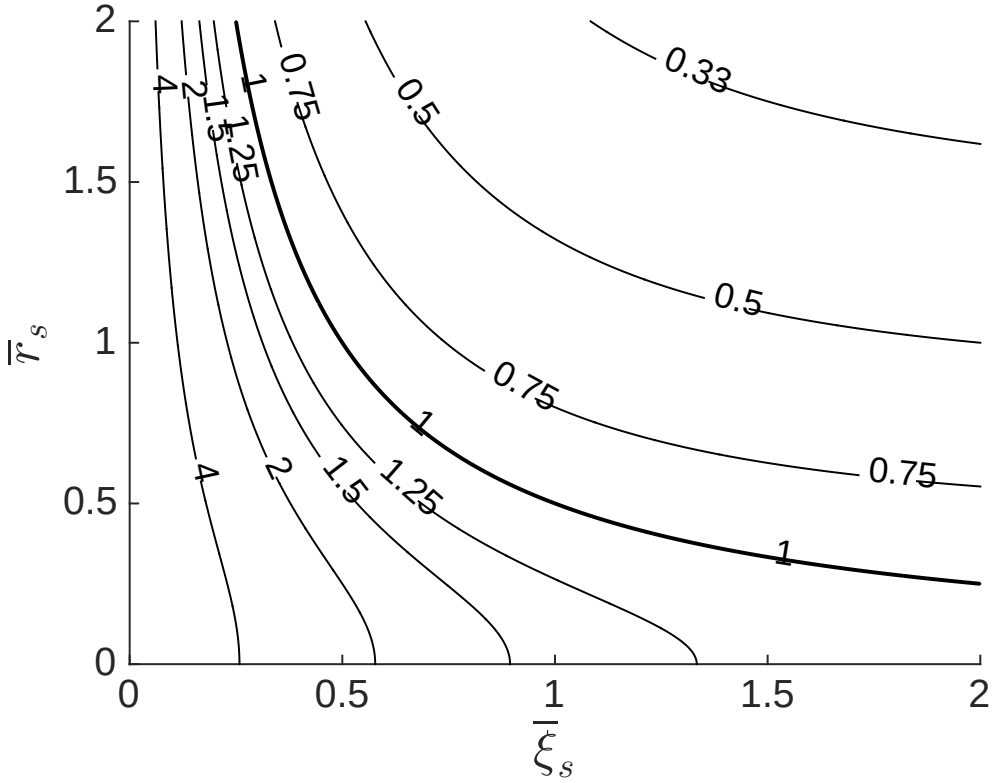

Contour levels of the coefficient of variation of the smoothed Wigner transform. Here $\overline{r}_{\rm s} = r_{\rm s}/\rho_z$ and $\overline{\xi}_{\rm s} = \xi_{\rm s}\rho_z$.

Application 1: Imaging below an "overburden"

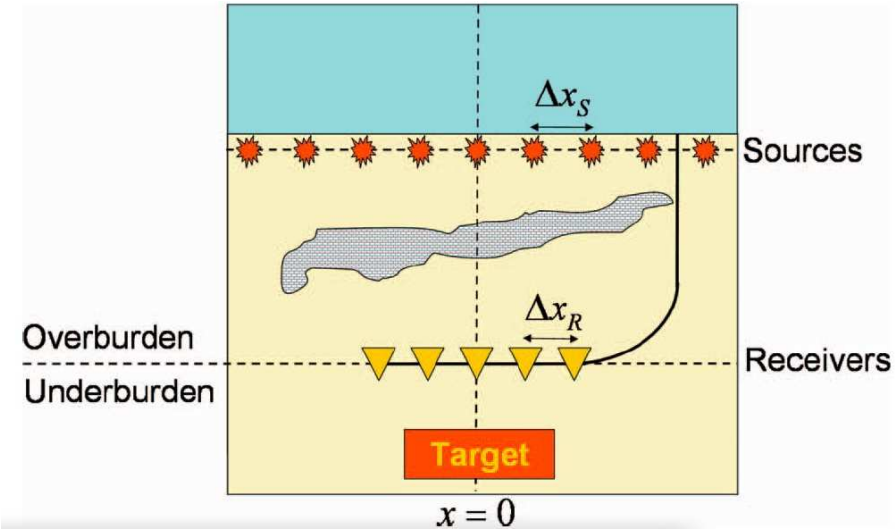

From van der Neut and Bakulin (2009)

Imaging below an overburden

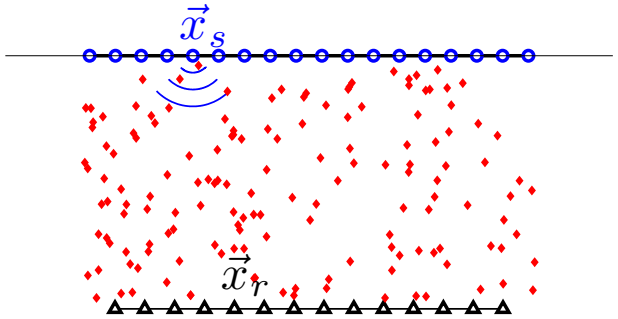

Array imaging of a reflector at $\vec{\boldsymbol{y}}_{\rm ref}$. $\vec{\boldsymbol{x}}_s$ is a source, $\vec{\boldsymbol{x}}_r$ is a receiver located below the scattering medium. Data: $\{u(t, \vec{\boldsymbol{x}}_r; \vec{\boldsymbol{x}}_s), r = 1, \ldots, N_{\rm r}, s = 1, \ldots, N_{\rm s}\}$.

If the overburden is scattering, then Kirchhoff Migration does not work:

$$\mathcal{I}_{\rm KM}(\vec{\boldsymbol{y}}^S) = \sum_{r=1}^{N_{\rm r}} \sum_{s=1}^{N_{\rm s}} u\Big(\frac{|\vec{\boldsymbol{x}}_s - \vec{\boldsymbol{y}}^S|}{c_o} + \frac{|\vec{\boldsymbol{y}}^S - \vec{\boldsymbol{x}}_r|}{c_o}, \vec{\boldsymbol{x}}_r; \vec{\boldsymbol{x}}_s \Big)$$

Numerical simulations

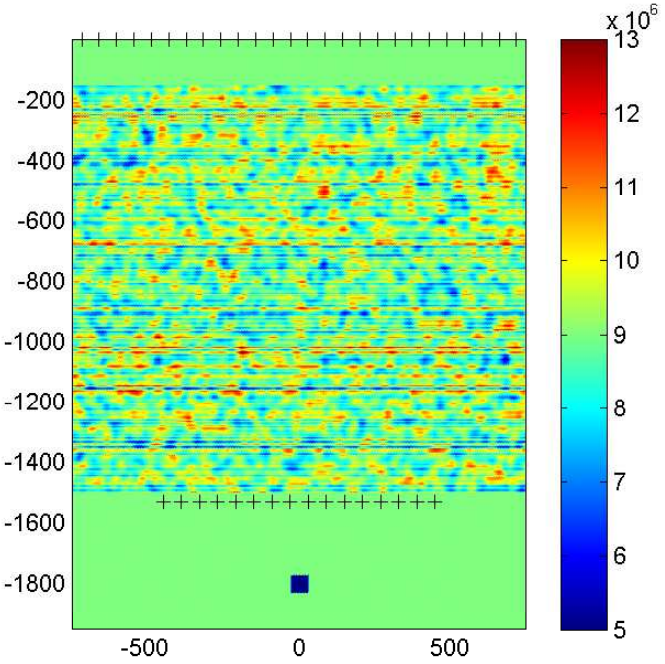

Computational setup

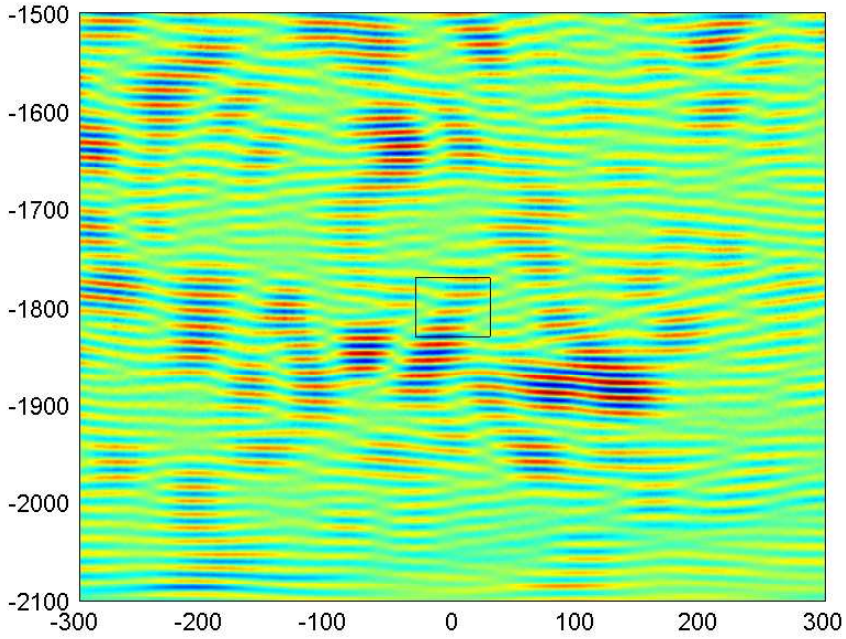

Kirchhoff Migration

(simulations carried out by Chrysoula Tsogka, University of Crete)

Imaging below an overburden

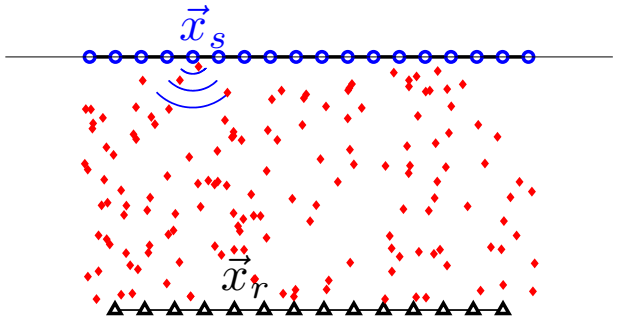

$\vec{y}_{ref}$

$\vec{\boldsymbol{x}}_s$ is a source, $\vec{\boldsymbol{x}}_r$ is a receiver. Data: $\{u(t, \vec{\boldsymbol{x}}_r; \vec{\boldsymbol{x}}_s), r = 1, \ldots, N_{\rm r}, s = 1, \ldots, N_{\rm s}\}$.

Image with migration of the special cross correlation matrix:

$$\mathcal{I}(\vec{\boldsymbol{y}}^S) = \sum_{r,r'=1}^{N_{\rm r}} \mathcal{C}\Big(\frac{|\vec{\boldsymbol{x}}_r - \vec{\boldsymbol{y}}^S|}{c_o} + \frac{|\vec{\boldsymbol{y}}^S - \vec{\boldsymbol{x}}_{r'}|}{c_o}, \vec{\boldsymbol{x}}_r, \vec{\boldsymbol{x}}_{r'}\Big),$$

with

$$\mathcal{C}(\tau, \vec{\boldsymbol{x}}_r, \vec{\boldsymbol{x}}_{r'}) = \sum_{s=1}^{N_{\rm s}} \int u(t, \vec{\boldsymbol{x}}_r; \vec{\boldsymbol{x}}_s) u(t+\tau, \vec{\boldsymbol{x}}_{r'}; \vec{\boldsymbol{x}}_s) dt \ , \qquad r, r' = 1, \ldots, N_{\rm r}$$

Related to CINT (Borcea, Papanicolaou, Tsogka), imaging with ambient noise sources (Campillo, Garnier and Papanicolaou), virtual source method (Bakulin and Calvert).

Remark: General CC function (with $\hat{u}(\omega, \vec{\boldsymbol{x}}_r; \vec{\boldsymbol{x}}_s) = \int u(t, \vec{\boldsymbol{x}}_r; \vec{\boldsymbol{x}}_s) e^{-i\omega t} dt$):

$$\mathcal{I}_{\rm CC}(\vec{\boldsymbol{y}}^S) = \sum_{\substack{s,s'=1 \\ |\vec{\boldsymbol{x}}_s - \vec{\boldsymbol{x}}_{s'}| \le X_{\rm d}}}^{N_{\rm s}} \sum_{\substack{r,r'=1 \\ |\vec{\boldsymbol{x}}_r - \vec{\boldsymbol{x}}_{r'}| \le X'_{\rm d}}}^{N_{\rm r}} \iint_{|\omega - \omega'| \le \Omega_{\rm d}} d\omega d\omega' \, \hat{u}(\omega, \vec{\boldsymbol{x}}_r; \vec{\boldsymbol{x}}_s) \overline{\hat{u}(\omega', \vec{\boldsymbol{x}}_{r'}, \vec{\boldsymbol{x}}_{s'})}$$

$$\times \exp\Big\{ -i\omega \Big[\frac{|\vec{\boldsymbol{x}}_r - \vec{\boldsymbol{y}}^S|}{c_o} + \frac{|\vec{\boldsymbol{x}}_s - \vec{\boldsymbol{y}}^S|}{c_o} \Big] + i\omega' \Big[\frac{|\vec{\boldsymbol{x}}_{r'} - \vec{\boldsymbol{y}}^S|}{c_o} + \frac{|\vec{\boldsymbol{x}}_{s'} - \vec{\boldsymbol{y}}^S|}{c_o} \Big] \Big\}$$

- If $X_{\rm d} = X'_{\rm d} = \Omega_{\rm d} = \infty$, then $\mathcal{I}_{\rm CC}(\vec{\boldsymbol{y}}^S) = \big|\mathcal{I}_{\rm KM}(\vec{\boldsymbol{y}}^S)\big|^2$.
- If $X_{\rm d} = 0$, $X'_{\rm d} = \infty$, $\Omega_{\rm d} = 0$, then $\mathcal{I}_{\rm CC}(\vec{\boldsymbol{y}}^S)$ is the previous imaging function.
- In general, there are optimal values for $X_{\rm d}, X'_{\rm d}, \Omega_{\rm d}$ that achieve a good trade-off between resolution and stability.

Numerical simulations

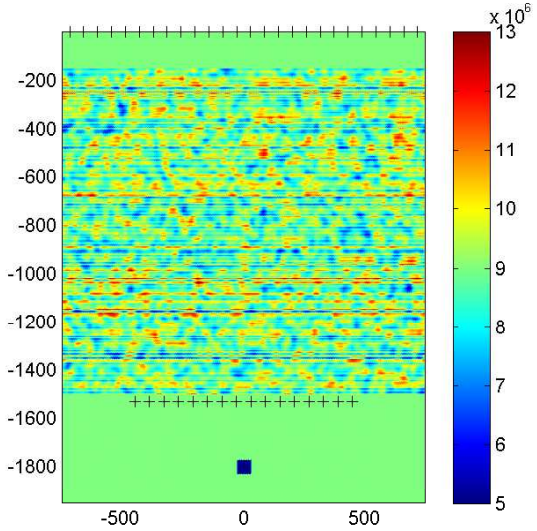

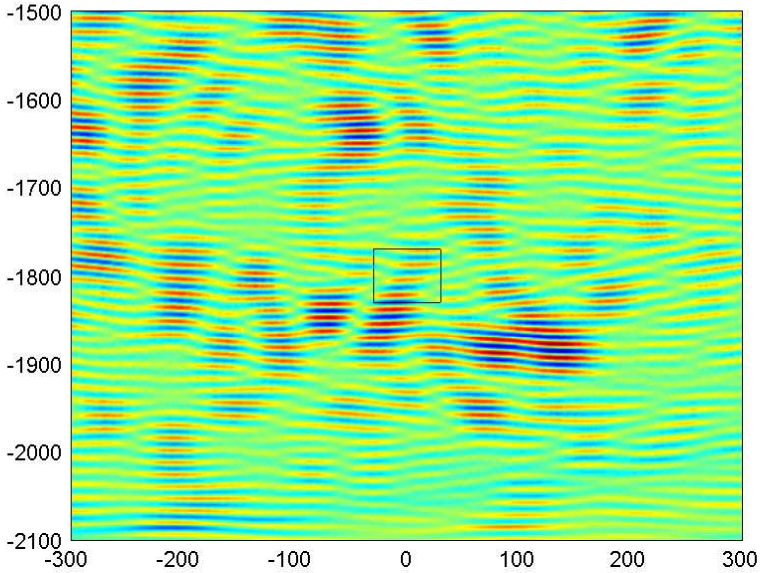

Kirchhoff Migration

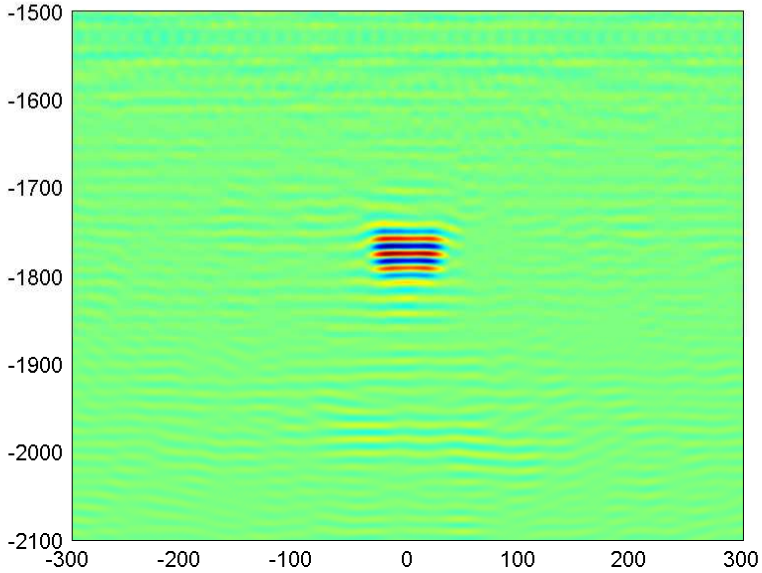

Correlation-based Migration

[1] J. Garnier, G. Papanicolaou, A. Semin, and C. Tsogka, *SIAM J. Imaging Sciences* **8**, 248 (2015).

Application 2: Ultrasound echography in concrete

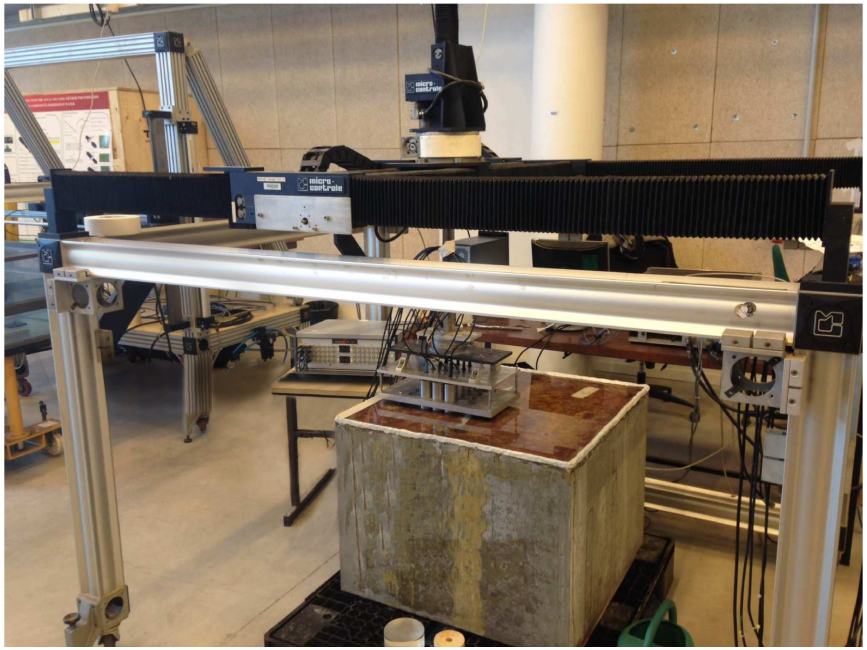

Experimental set-up

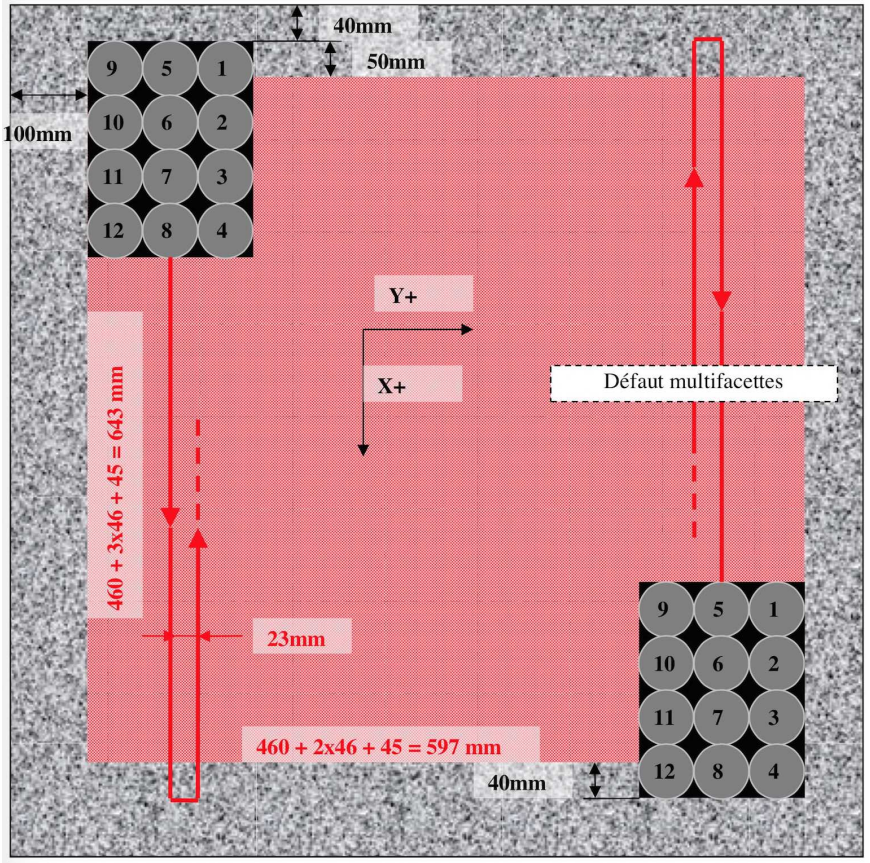

Acquisition geometry (top view)

Concrete: highly scattering medium for ultrasonic waves.

Ultrasound echography in concrete

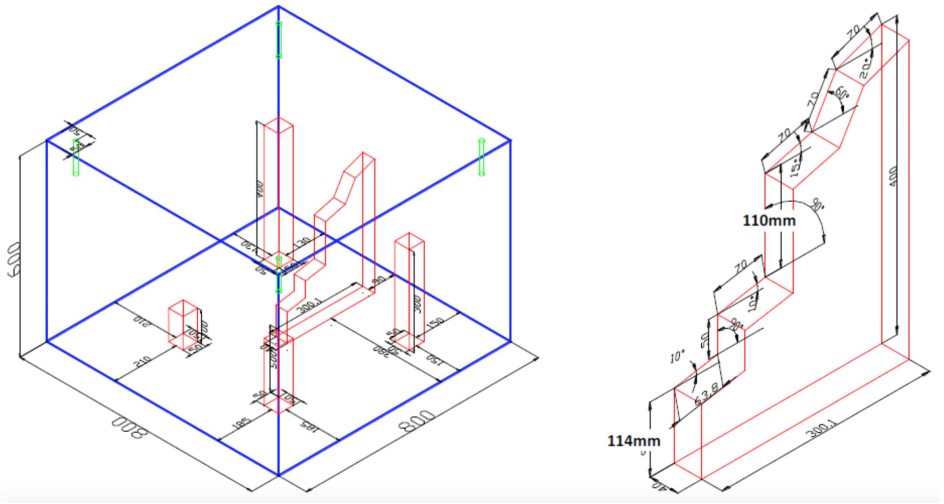

Real configuration

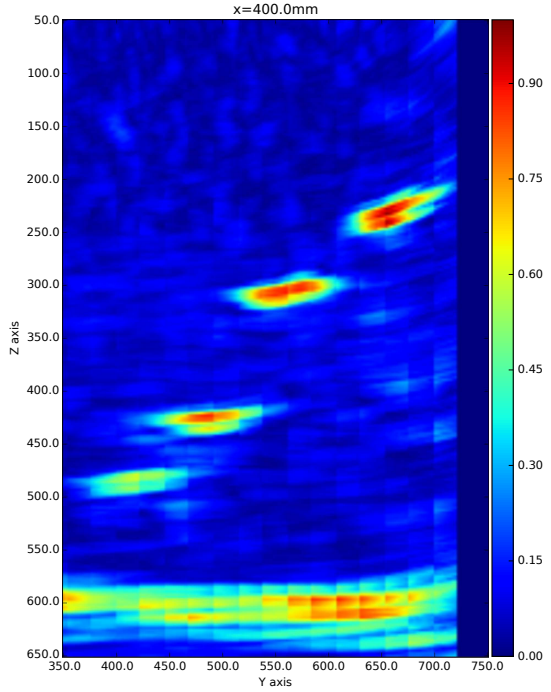

Image (2D slice)

Image obtained by travel-time migration of *well-chosen* cross correlations of data.

Ghost imaging

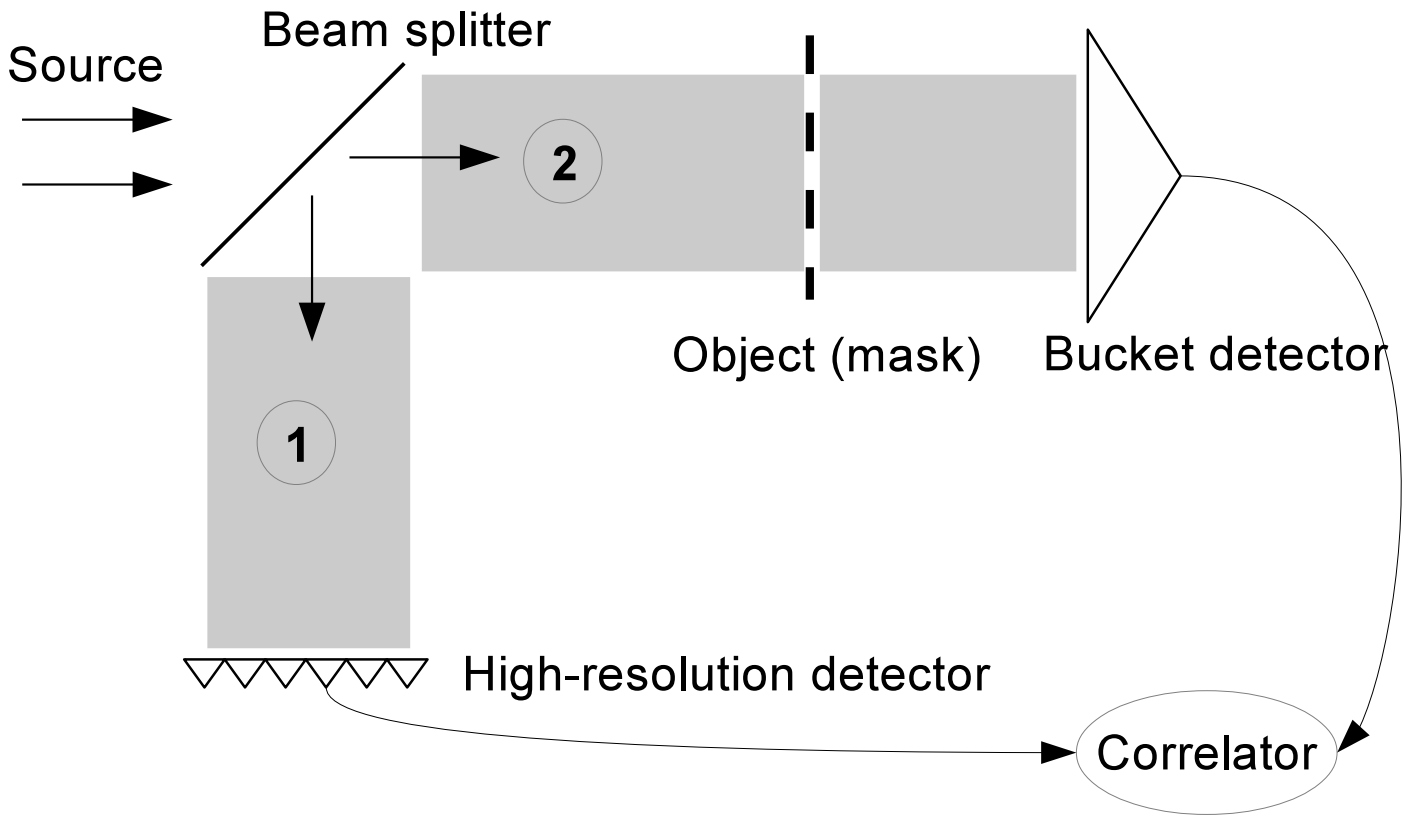

- Noise source (laser light passed through a rotating glass diffuser).
- without object in path 1; a high-resolution detector measures the spatially-resolved intensity $I_1(t, \boldsymbol{x})$.
- with object (mask) in path 2; a single-pixel detector measures the spatially-integrated intensity $I_2(t)$.

Experimental result: the correlation of $I_1(\cdot, \boldsymbol{x})$ and $I_2(\cdot)$ is an image of the object [1,2].

[1] A. Valencia et al., *PRL* **94**, 063601 (2005); [2] J. H. Shapiro et al., *Quantum Inf. Process* **1**, 949 (2012).

Ghost imaging

- Wave equation in paths 1 and 2:

$$\frac{1}{c_j^2(\vec{\boldsymbol{x}})}\frac{\partial^2 u_j}{\partial t^2} - \Delta_{\vec{\boldsymbol{x}}} u_j = e^{-i\omega_o t} n(t,\boldsymbol{x})\delta(z) + c.c., \qquad \vec{\boldsymbol{x}} = (\boldsymbol{x}, z) \in \mathbb{R}^2 \times \mathbb{R}, \qquad j = 1, 2$$

- Noise source (with Gaussian statistics):

$$\Big\langle n(t,\boldsymbol{x})\overline{n(t,\boldsymbol{x}')}\Big\rangle = F(t-t')\exp\Big(-\frac{|\boldsymbol{x}|^2}{r_o^2}\Big)\delta(\boldsymbol{x}-\boldsymbol{x}')$$

with the width of $\hat{F}(\omega)$ much smaller than ω_o.

- Wave fields:

$$u_j(t,\vec{\boldsymbol{x}}) = v_j(t,\vec{\boldsymbol{x}})e^{-i\omega_o t} + c.c., \qquad j = 1, 2$$

- Intensity measurements:

$$\begin{aligned} I_1(t,\boldsymbol{x}) &= |v_1(t,(\boldsymbol{x},L))|^2 \text{ in the plane of the high-resolution detector} \\ I_2(t) &= \int_{\mathbb{R}^2} |v_2(t,(\boldsymbol{x}',L+L_0))|^2 d\boldsymbol{x}' \text{ in the plane of the bucket detector} \end{aligned}$$

- Correlation:

$$C_T(\boldsymbol{x}) = \frac{1}{T}\int_0^T I_1(t,\boldsymbol{x})I_2(t)dt - \Big(\frac{1}{T}\int_0^T I_1(t,\boldsymbol{x})dt\Big)\Big(\frac{1}{T}\int_0^T I_2(t)dt\Big)$$

Ghost imaging

- Result:

$$C_T(\boldsymbol{x}) \overset{T\to\infty}{\longrightarrow} C^{(1)}(\boldsymbol{x}) \text{ deterministic and dependent on the mask function } \mathcal{T}$$

- If the propagation distance is larger than the scattering mean free path, then

$$C^{(1)}(\boldsymbol{x}) = \int_{\mathbb{R}^2} \mathcal{H}(\boldsymbol{x}-\boldsymbol{y})|\mathcal{T}(\boldsymbol{y})|^2 d\boldsymbol{y},$$

with

$$\mathcal{H}(\boldsymbol{x}) = \frac{r_o^4 \rho_{\text{gi0}}^2}{2^8 \pi^2 L^4 \rho_{\text{gi2}}^2} \exp\Big(-\frac{|\boldsymbol{x}|^2}{4\rho_{\text{gi2}}^2}\Big), \qquad \rho_{\text{gi2}}^2 = \rho_{\text{gi0}}^2 + \frac{4c_o^2 L^3}{3\omega_o^2 Z_{\text{sca}} \ell_{\text{c}}^2}, \qquad \rho_{\text{gi0}}^2 = \frac{c_o^2 L^2}{2\omega_o^2 r_o^2}$$

$\hookrightarrow$ Scattering only slightly reduces the resolution !

This imaging method is robust with respect to medium noise. It gives an image even when $L/Z_{\text{sca}} \gg 1$.

Ghost imaging with a virtual high-resolution detector

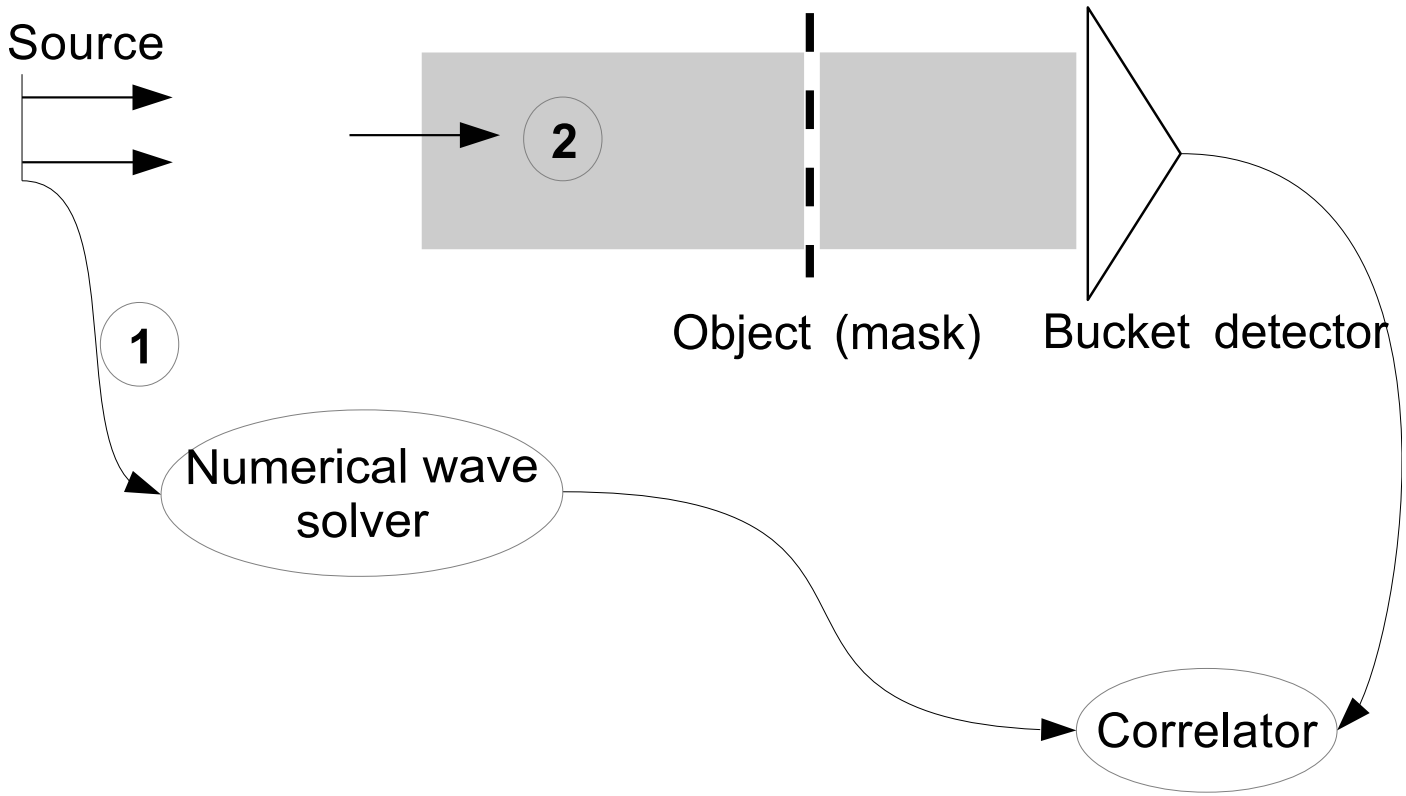

- The medium in path 2 is randomly heterogeneous.
- There is no other measurement than the integrated transmitted intensity $I_2(t)$.
- The realization of the source is known (use of a Spatial Light Modulator) and the medium is taken to be homogeneous in the "virtual path 1" $\rightarrow$ one can *compute* the field (and therefore its intensity $I_1(t, \boldsymbol{x})$) in the "virtual" output plane of path 1.

$\hookrightarrow$ a *one-pixel camera* can give a high-resolution image of the object!

Conclusion

- First and second-order moments of the wave field:
- Application: Correlation-based imaging in randomly scattering media.

One needs to process *well-chosen* cross correlations of the data.

- Fourth-order moments of the wave field.
- First application: Scintillation index and stability of Wigner transform.
- Second application: Intensity correlation-based imaging, ghost imaging.
- Hopefully, many other applications !